Article:
Mistry, D orcid.org/0000-0003-0012-6781, Traugutt, NA, Yu, K et al. (1 more author) (2021) Processing and reprocessing liquid crystal elastomer actuators. Journal of Applied Physics, 129 (13). 130901. ISSN 0021-8979

https://doi.org/10.1063/5.0044533

Processing and Reprocessing Liquid Crystal Elastomer Actuators

Devesh Mistry[1], Nicholas Traugutt[1], Kai Yu[1], Chris Yakacki[1]

[1]*Department of Mechanical Engineering, University of Colorado, Denver, Denver, 80203, USA*

Abstract

Liquid crystal elastomers have long been celebrated for their exceptional shape actuation and mechanical properties. For much of the last half century, a major focus for the field has been the development of LCE chemistries and how to process so-called "monodomain" configurations. This foundation work has now led to a plethora of materials and processes which are enabling demonstration of devices which are close to real-world applicability as responsive and reprocessable actuators. In this perspective, we review and discuss the key recent developments in the processing of actuating LCE devices. We consider how processing has been used to increase the practicality of electrical, thermal, and photo stimulation of LCE shape actuation; how dynamic chemistries are enhancing the functionality and sustainability of LCE devices; and how new additive manufacturing technologies are overcoming the processing barriers that once confined LCE actuators to thin-film devices. In our outlook, we consider all these factors together and discuss what developments over the coming years will finally lead to the realization of commercial shape actuating LCE technologies.

I. Introduction

Since their conception 50 years ago, liquid crystal elastomers (LCEs) have long promised bioinspired actuating mechanical devices. Application areas are diverse and include robotics, photonics, medical, and aerospace industries.[1–9] Undoubtedly, there has been no limit to the research community's imagination in proposed devices and technologies. However, despite the range of prototype devices demonstrated thus far, no commercial LCE devices have been brought to market. The historical challenges associated with developing versatile and facile LCE chemistries, and adequate processing methods appear to be largely solved. The remaining barriers to realizing commercial actuating LCE devices now lie in developing effective powering strategies for stimulating actuation and ensuring devices are synthesized from reprogrammable and recyclable materials. This perspective focuses on the recent key developments in the processing and reprocessing of LCE devices that are pushing the field closer to the realization of commercialized actuating LCE technologies. We also provide outlook on the remaining challenges to LCE commercialization and how they may be approached in the next 5 years.

Since the advent of click-chemistry LCEs in 2015, LCE synthesis has become somewhat routine as researchers across disciplines can successfully synthesize LCEs in-house with relative ease and from commercially available chemicals. In particular, with thiol-acrylate Michael addition and thiol-ene click-chemistries, one can easily prepare a diverse range of optimized and functionalized LCEs through careful choice of the dithiol spacer groups used.[10–12] For instance, by choosing dithiol alkyl spacers, one can introduce dynamic crystallinity – a phenomenon with application potential in biomedical devices such as spinal fusion cages and stents.[1,10,13]

In addition, by including groups such as allyls, disulfide bridges, siloxanes, and boronic esters, one can develop dynamic bond exchange and vitrimer networks that introduce adaptability and recyclability to LCEs.[12,14–16] Recent reviews by Ula *et al.,* Wang *et al.* and Saed *et al.* provide a deep insight into the various LCE synthesis routes and strategies for achieving adaptable and recyclable networks.[4,17,18] In dynamic networks, the ability to break, reform, or exchange crosslinks or chains means that, in principle, a LCE's network architecture and actuation capability can be forever re-defined.[11,14] Moreover, through surface welding effects, such dynamic chemistries allow the lamination an LCE actuator with LCE actuators of different chemistries or functionalities or with distinct polymeric materials of different functionalities.[19] Thus, dynamic chemistries offer an exciting spectrum of additional ways in which to process and reprocess LCE-based devices.

Many of the exciting properties of LCEs, namely reversible shape actuation, become possible when "monodomain" configurations are prepared.[20] A monodomain exists when the direction of local liquid crystal alignment – the director – is macroscopically aligned between neighboring domains. As such, the processing of aligned monodomain LCEs has long been a central focus of the LCE research community. Of particular interest has been devices prepared with spatially varying director profiles (e.g., concentric circles and spirals), which switch between Gaussian and non-Gaussian curvatures when actuated and thus can generate out-of-plane forces.[21–24]

Until 2014, monodomain LCEs were almost exclusively processed via either two-stage mechanical alignment,[25,26] surface alignment,[21,27,28] or magnetic field alignment.[29,30] With two-stage mechanical alignment, a lightly crosslinked macroscopically disordered (polydomain) LCE is aligned into a monodomain by applying a (typically) uniaxial mechanical strain – a state locked in by the subsequent formation of additional crosslinks. With surface alignment and magnetic field alignment, a nematic monomer or oligomer precursor is first aligned, and then the crosslinked network is formed through polymerization. At first glance, these various synthesis routes achieve similar end products; however, the route to synthesis will impact the physical properties and mechanical properties of the final materials.[31]

A major limitation of these processing routes is that while they can produce large sheets of monodomain LCE, they are restricted to thin film of typically <0.5 mm thick. 3D shapes can be achieved from 2D films through techniques such as forming/molding, network establishment at elevated temperatures, and surface welding components together, however these devices are still ultimately planar in nature and the range of 3D shapes possible is limited.[19,32]

Since 2014, additive manufacturing techniques have emerged for the preparation of intricate 3D and bulk 3D LCE devices. A two-photon polymerization process first reported by Zeng *et al.* is capable of "writing" microscopic 3D devices through selective polymerization of nematic acrylate monomer precursors which are aligned in a traditional LC cell device.[33] By contrast, the more recent direct-ink-writing (DIW) 3D-printing approach, which typically deposits filaments of shear aligned photo-crosslinkable LC oligomer, can produce the largest monodomain LCE devices prepared to date.[34–36] Most recently, digital light process (DLP) 3D-printing has fabricated highly intricate polydomain LCE lattices and monodomain glassy liquid crystal (LC) networks, with the monodomains networks aligned *via* magnetic fields.[13,30,37]

As highlighted in Ambulo *et al.'s* recent review on LCE processing for biomedical device applications, each of the various LCE processing routes developed over the years offers its own advantages and drawbacks to the possible resolution of physical features, resolution of director patterning, and ultimate size of prepared devices.[38] Common with many materials processing routes, high resolution comes at the prices of device size.

The use of LCEs as soft actuators is appealing for several reasons. Unlike many other soft (e.g., pneumatic) and hard (e.g., electrical motor) actuating systems, the LCE material is the actuator itself. This simultaneity of being both the driven actuating element and driving the actuation means that LCE's functionality is highly reminiscent of biological muscle tissues. If energy and stimulus can be effectively delivered in devices, then the actuator can perform its function. This allows for compact actuators, which can also be entirely passive and respond to their environment.[5,39] In actively-driven LCE devices, effective delivery of a stimulus, whether by thermal, optical, or chemical means, remains the primary challenge. Given the apparent similarities with muscle tissues, LCE actuators' performance is often compared against that of mammalian skeletal muscles. Broadly speaking, mammalian skeletal muscles are capable of actuation strains on the order of 20%, work densities on the order of 50 kJ m^{-3}, work capacities of ~50 J kg^{-1}, and actuation times on the order of 1 s.[40,41] Moreover, through the adoption of dynamic and adaptable network chemistries, LCE devices show the promise of mimicking the adaptable and self-healing characteristics of biological tissues. These fundamental capabilities of LCEs have long being celebrated, going forward, the challenge is processing functional devices from these promising materials.

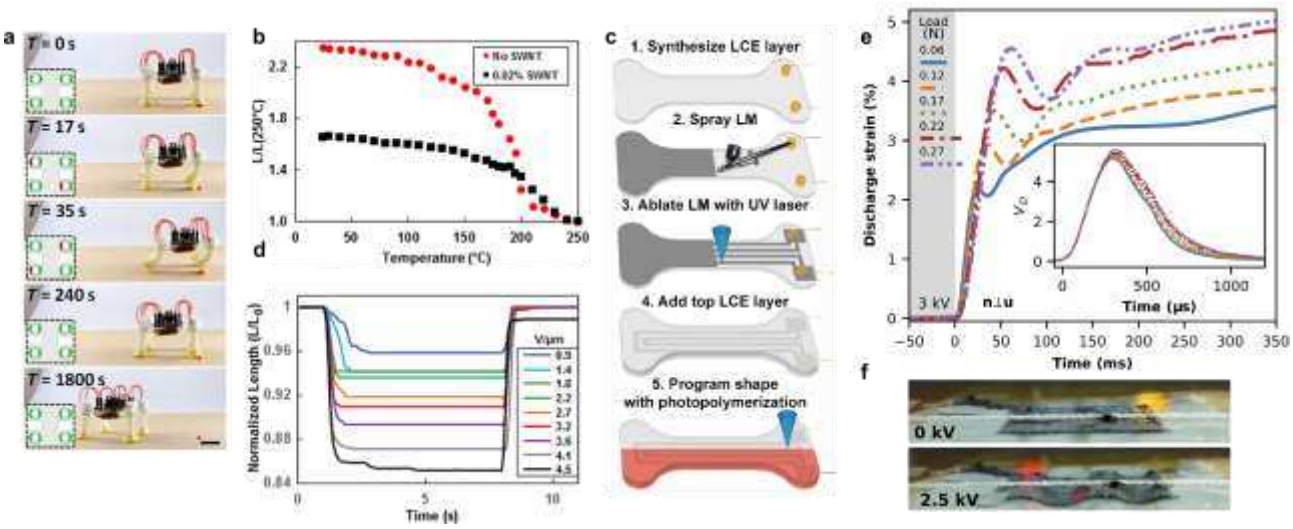

Figure 1 a *He et al.'s demonstration of an entirely standalone soft robotic LCE device based on Joule heated tubular actuators. Reprinted from He et al., Sci. Adv.* ***5****, eaax5746 (2019). © The Authors, some rights reserved; exclusive licensee AAAS. Distributed under a Creative Commons Attribution NonCommercial License 4.0 (CC BY-NC).* ***b*** *The inclusion of SWCNTs in monodomain LCEs restricts and diminishes the strain actuation magnitude achieved. Reprinted with permission from Guin et al. ACS Appl. Mater. Interfaces,* ***10****, 1187 (2018). Copyright 2021 American Chemical Society.* ***c*** *Kent et al.'s illustration of how joule-heated liquid metal LCE actuators are fabricated. Reprinted with permission from Kent et al. Multifunc. Mater.,* ***3****, 025003 (2020). Copyright 2021 Institute of Physics, DOI: 10.1088/2399-7532/ab835c.* ***d*** *LCEs can be actuated via the electroconstriction effect, but large actuation strains require large voltages. Reprinted with permission from Guin et al. ACS Appl. Mater. Interfaces,* ***10****, 1187 (2018). Copyright 2021 American Chemical Society.* ***e*** *Dielectric LCE actuators demonstrate fast actuation times, and* ***f*** *can used to achieve out of plane deformations if constrained along their actuation direction. Reprinted from Davidson et al., Sci. Adv.* ***5****, eaay0855 (2019). © The Authors, some rights reserved; exclusive licensee AAAS. Distributed under a Creative Commons Attribution NonCommercial License 4.0 (CC BY-NC).*

In this perspective, we discuss recent papers, particularly those from the last two years, which in our view report key developments the processing and reprocessing of LCEs taking the field closer to realizing commercial actuating devices in the next 3-6 years. We also explore what barriers remain in the pursuit of actuating LCE devices and how these may be overcome in the coming years.

II. Stimulating actuation

A. Processing for electrical stimulation

Arguably, electrical stimulation is ideal for triggering LCE actuation as the transmission of both power and signals over electrical wires has long been trivial. Recently, the first standalone and untethered LCE robotic device was created using Joule heated tubular actuators. [Fig. 1(a)].[42] This device was made possible by the relatively recent availability of low cost and lightweight programmable microcontrollers. Over the years, several distinct modes for electrically stimulating actuating muscle-like LCEs have been developed. This includes dipole-induced rotation/electrostrictive effects in carbon nanotube-doped LCEs, electric field-Fréedericksz effects in LCEs swollen with low molecular mass LCs, Maxwell stresses in dielectric LCE actuators, and Joule heating.[29,43–51]

Joule heating is perhaps the simplest form of electrical-based stimulation. It can be achieved either through embedded solid or liquid metal conductors or through the formation of carbon nanotube- or liquid metal-composites. However, Joule heating is not without its limitations, such as the reliance on passive cooling for reverse actuation, wires or composite particles restricting actuation strains [Fig. 1(b)] and causing delamination, and slow actuation rates (particularly in bulk devices).[43,45] One approach to avoid delamination effects is to use

liquid metal conductors.[50–52] Kent *et al.* recently demonstrated that such liquid metal conductors in LCE actuator devices can also be used as thermistor-like sensors to enable closed-loop temperature control of the LCE [Fig. 1(c)].[51] However, the authors also noted that in LCEs actuated via Joule heating, care is needed to mitigate the effects of electromigration, which can cause the failure or shorting of electronic devices.

LCE actuation *via* the electrostrictive effect was shown by Guin *et al.* who reported a facile blade coating approach to prepare large (e.g., 10 cm x 100 cm x 100 µm) films of monodomain LCEs doped with carbon nanotubes (CNTs).[45] For thin-film devices, the voltages required to actuate these films (~0.5 V μm^{-1}) are compatible with common household voltages. While the processing approach is evidently capable of industrial-scale production, the response time of the actuation (~10 s) and strains achievable via electrostriction (~1.25% without inducing plastic deformation) may in practice limit the applicability of LCE devices actuated via electrostriction [Fig. 1(d)].

The direction(s) in which a LCE actuates in response to an electrical stimulation depends upon which physical effect is being used. In the works of Courty *et al.*, Guin *et al.* (for LCEs doped with CNTs), and Urayama (an LCE swollen with a low molecular mass LC), an electric field is applied perpendicular to the director of a monodomain films of LCE and, although the physical actuating mechanisms differ, the result is a rotation of the director toward the applied field and a thus a contraction of the LCE along the initial director orientation axis.[43,44,46] These methods have nuanced differences from actuations triggered by Joule heating, in which an LCE device actuates *via* contractions (expansions) parallel (perpendicular) to a fixed director.[20,29] Z. Davidson *et al.* recently described an additional mode of electrical actuation using a monodomain LCE in a dielectric actuator.[48] Here, the use of an anisotropic LCE dielectric (with the director in plane of the LCE film) leads to an anisotropic dielectric actuation which is almost entirely confined to the axis perpendicular to the applied field and director (i.e. the direction of soft elasticity). Interestingly, this actuation is, for a given Maxwell stress, twice as large as those seen in isotropic dielectric elastomers. A key advantage of the dielectric elastomer approach to LCE actuation is the speed of actuation. For example, for a sample pre-loaded with ~50 kPa, actuation strains perpendicular to the director of ~3% are seen within ~100ms of a 3 kV stimulating voltage being applied, with ~5% achieved after 4 seconds. On discharge, the actuation response within 100 ms appears similar, however, a 1 % strain remains after 2 seconds– a phenomenon attributed to the highly viscous nature of LCEs [Fig. 1(e)]. The authors also demonstrated using constrained devices [Fig. 1(f)] and patterned director profiles to generate non-Gaussian curvature and out of plane deformations. But, such devices' ability to lift loads has not yet been assessed nor compared against the impressive performances of director-patterned, thermally actuated LCE devices. Moreover, as common with isotropic dielectric elastomers, actuations require high (~kV) voltages which may be impractical.

If we turn away from large-scale muscle-like actuators, Liu *et al.* and Feng *et al.* have described electric fields being successfully employed to create spatially and temporarily periodic undulating actuations in LC network coatings – which could for instance be applied to haptics and self-cleaning surfaces.[6,53] These works use nematic and chiral nematic LC networks coated on top of microscopic interdigitated electrodes. When continuous alternating electric fields of amplitude ~75 V and frequencies between ~0.5-1 MHz are applied, the surfaces develop a micron-scale periodic surface topology (determined by the periodicity of the electrodes and the chiral nematic pitch length) with a height amplitude ≤6% of the initial film thickness. For example, ~150 nm high undulations were seen in a film of 2.5µm thickness.[53] These effects are driven by the electric fields causing reductions of the LC order parameter which increases the free volume of the network. As the deformations are constricted by the substrate the films are bonded to, they are forced to protrude out of plane. The generated topologies also exhibit oscillations chaotic with time and which are thought to be linked to the sensitivity of the network's resonance to the changing geometry and modulus. In both cases, the amplitude of the spatial and temporal oscillations is maximized when the coating is held close to its glass transition temperature - implying the behavior could be enhanced through the use of LCEs. Feng *et al.* demonstrated that the response in a chiral nematic coating would aid the removal of dirt from surfaces in arid environments. While both works suggest the coatings would be applicable to haptics, it seems likely that further work will be needed to optimize materials to enhance the height amplitude of the surface

features and reduce the voltages required. In terms of processing active and dynamic coatings such as those described above benefit from the wealth of materials, technologies and processes developed in LCDs research.

B. Processing for photo-stimulated actuation

The most common photothermal actuation mechanism sees LCEs doped with CNTs being heated *via* absorption of infra-red light.[38,49,54] As with Joule heated LCEs, reverse actuation relies on the passive cooling of a device which can limit applicability. Liu *et al.* recently reported the production of LCE composite fibers filled with CNTs and cellulose nanocrystals.[49] In addition to Joule heating, the actuation can be triggered through the photothermal effect. The authors also showed that through additional inclusion of cellulose nanocrystals, the strength and work capacity of the LCE fibers increased to better match the performance of conventional "hard" actuators. The increase in work capacity was attributed to the shearing of the cellulose nanocrystals during fiber extrusion facilitating greater LC alignment. The authors also found that the extrusion processing allowed for up to a 2 wt. % loading of homogeneously dispersed CNTs – far greater than that reported by previous studies which found aggregation of CNTs for loadings greater than 0.1 wt. %. Furthermore, when fibers were bundled together, they were capable of work capacities of 55 J kg^{-1} – favorable compared to the ~40 J kg^{-1} of human muscle. Despite this, the actuation strain possible (6%) was significantly lower than one would expect from LCEs and the actuator's response time (~30 s) is likely to be slower than needed for many applications.

A photo-chemical/thermal response can also be achieved with the use of dyes containing azobenzene groups.[33,55–57] Upon UV irradiation, the switching from *trans* (planar) to *cis* (non-planar) isomers upon UV radiation reduces LC order due to photo-thermal heating and the shape of the cis isomer disrupting LC order. Reverse actuation requires the relaxation of *cis* isomers back to the *trans* isomers. This can be achieved thermally – via the heat generated during UV exposure and actuation, or optically by exposure to blue wavelengths of light (a slower process than *trans* to *cis* isomerization via UV light).[57] For dyes with a sufficiently fast cis to trans relaxation time and a film-like device (able to quickly dissipate heat to the environment), such systems are capable of >1 Hz actuation cycles.[58] Thicker devices are challenged by the longer time needed to dissipate heat and the exponential decay in UV light penetration, which can cause unwanted bending deformations.

To date, photo-chemical based LCE actuators have been somewhat limited to thin-film devices. While untethered photo-response LCE actuators are sometimes claimed, we would argue that these only exist in devices designed to passively respond to environmental stimuli, for instance Zeng *et al.'s* self-regulating flower-like iris device.[5] For actively driven devices, the control hardware and light source(s) providing stimuli are external to the actuating device. With currently published research, it is likely that the control hardware and light source(s) would be much too large and massive to be incorporated into a truly standalone and untethered photo-responsive soft robotic device. In principle, photo-stimulated actuation is an attractive method for actively driven devices as the transport of light is fast, efficient, and easily spatially and temporally modulated. Moreover, if actuation can be achieved with a minimal temperature increase and reverse actuation can be effectively stimulated, photo-actuated devices could be superior to Joule heated LCE devices. However, the main challenge of achieving actuation in a bulk photo responsive LCE actuator would still need to be overcome.

III. Dynamic and recyclable chemistries

Conventional LCEs exhibit permanently crosslinked networks and therefore their shape and actuation behaviors are fixed. However, LCE networks with adaptable and reconfigurable functionality and mechanical performance can be created by exploiting several dynamic chemistries that have been recently developed.

To date, dynamic chemistries can be broadly classified into two groups. The first, based on reversible bonds built into the elastomer chain backbone (*e.g.*, Diels–Alder adducts), enables the breaking and reforming of polymer chains. Depending on the intensity of the stimulus, the rates at which the reversible bonds cleave and reconnect change to achieve dynamic equilibrium. The second uses bond exchange reactions (BERs) in which a chain connection event is immediately followed by a chain cleavage at the same site to maintain the overall network

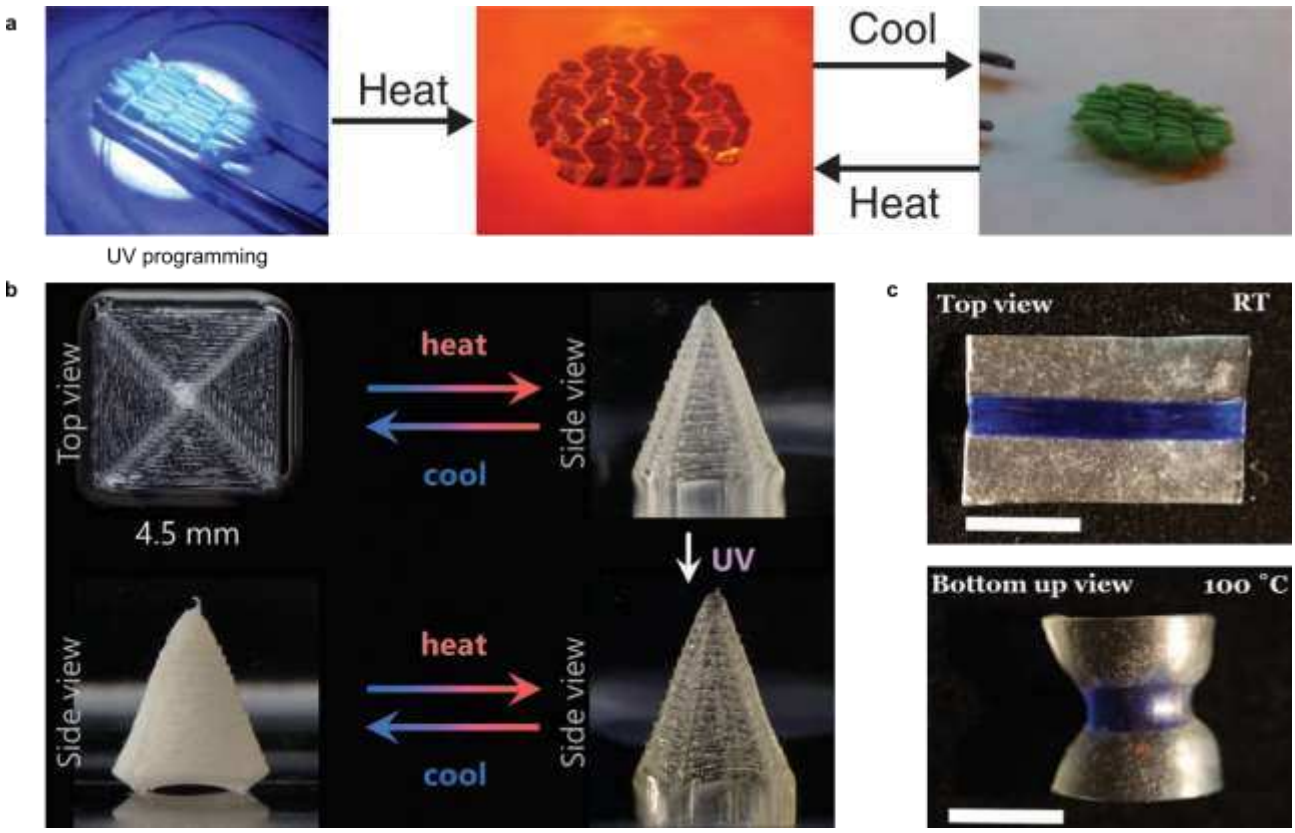

Figure 2 a *A flat LCE sheet is folded into the Miura pattern and programmed with BERs under UV irradiation to enable the reversible shape changing. Reprinted from McBride et al., Sci. Adv.* ***4****, eaat4634 (2018). © The Authors, some rights reserved; exclusive licensee AAAS. Distributed under a Creative Commons Attribution NonCommercial License 4.0 (CC BY-NC).* ***b*** *The reversible shape-changing of a 3D printed LCE sheet is deleted after UV irradiation to induce BERs. Reproduced with permission from Davidson et al., Adv. Mater.* ***32****, 1905682 (2020). Copyright 2020 Wiley* ***c*** *Shape changing of a bilayer film prepared by welding a programmed adaptable LCE strip (blue) with non-LCE strips (transparent). Reproduced with permission from Saed et al., Adv. Func. Mater.* ***30****, 1906458 (2020). Copyright 2020 Wiley.*

chain density. Various dynamic chemistries have been employed to create BER systems. Examples include radical-based chain transfer[59,60], transesterification[61,62] , imine exchange[63,64], and disulfide exchange[65,66]. A detailed review of the dynamic chemistries employed in adaptable LCEs can be found in Refs 17 and 18.

A major benefit of including dynamic chemistries in LCEs is that they enable a transformative and reprocessable actuator material as BER-induced creep flow can be used to modulate the mesogen orientation and program monodomain LCEs with reversible shape-changing.[11,12,14,16,32,67]. For example, Ji *et al.* reported the first thermal-responsive adaptable LCE with transesterification BERs[32] . In their system, monodomain LCEs were programmed by holding the specimens under a constant stress at temperatures above the BER-activation temperature (>160°C). In doing so, the polymer chains gradually aligned in the direction of the applied stress. By unloading samples at room temperature (far below the BER activation temperature), monodomain samples were obtained. A unique advantage of BER-assisted reprocessing is that the method can program non-trivial shape changes using either a non-uniform temperature, stress, or even light fields. For example, McBride *et al.* incorporated, into the chain backbone, functional groups capable of undergoing light-sensitive reverse addition-fragmentation chain transfer (RAFT) reactions which enable the spatial programming of LCEs with complex shapes.[14] Fig. 2(a) shows an example of an initially flat LCE film which was decorated with opaque tiles and folded into the Miura pattern. Upon

programming *via* irradiation to UV/visible light (320 to 500 nm), the LCE was programmed to hold the Miura pattern and would reversibly actuate to a flat sheet upon heating and cooling.

Using dynamic LCE chemistries, the mesogen alignment and shape-switching memory of monodomain LCEs can also be entirely deleted by activating enough random BERs to allow complete relaxation of the network. As a result, monodomain samples eventually return to the polydomain state and, if desired, can be reprogrammed.[11,12,32,68–71]. Wang *et al.* demonstrated this behavior *via* the inclusion of exchangeable disulfide bonds into the LCE network.[69] The obtained LCE could be reprogrammed into a monodomain state either under UV light or upon heating to 180°C. The reprogramming of adaptable LCEs was also demonstrated by Jiang *et al.*, wherein the Diels–Alder adducts were incorporated within the network. The programmed alignment in the LCE could be erased upon heating above the retro-addition reaction temperature of Diels–Alder adducts and reprogrammed again at room temperature. In the recent work by E. Davidson *et al.*, adaptable shape-changing LCEs with RAFT were fabricated using DIW 3D printing.[71] Fig. 2(b) shows that the reversible shape-changing of a 3D printed LCE sheet is deleted after UV irradiation to induce BERs under UV light.

Dynamic LCE networks can also exhibit surface welding effects, where physically separate samples are placed together, and polymer chains can be activated to covalently connect to each other on the interface. This effect can be utilized to assemble LCE structures with complex shape-changing. For example, Saed *et al.*, developed adaptable LCEs with dynamic exchangeable boronic esters.[16] A bilayer thin film was prepared by welding a programmed adaptable LCE strip (blue) with non-LCE strips with the same dynamic chemistry [Fig 2(c)]. Upon heating the welded structure, the bilayer device morphs into a half-tube shape with a negative Gaussian curvature – caused by the mismatch of local deformation between the two layers. Additionally, Zhang et al. used the surface welding-effect to create 3D structures from LCE films of different chemistries and hence actuating properties. The authors were able to create bio-inspired devices comprising components that were individually programmed to display bending, rotating, and stretching actuations prior to the final device was surface welded together.[19] The interfacial welding of adaptable LCEs can also be used to repair or recycle LCEs after damage – substantially improving the reliability and service life of LCEs.[11,16,32,69,72–74]

An excellent example of the capabilities of dynamic LCE networks was provided by He *et al.*, who recently used a disulfide bond exchange chemistry to improve upon their previous actuator device which is actively heated and cooled *via* pumped water.[75] In their work, the authors used a creep-aligned, bond-exchangeable LCE, laminated and self-welded together in three layers. Prior to assembly, the middle layer of the laminate was cut as to create channels throughout the final device. Using control hardware to pump water from either hot or cold reservoirs through the LCE device, the authors could cyclically heat and cool the LCE device between 20°C and 90°C at a frequency of 0.25Hz, with the device undergoing cyclical actuation strains of 30% (length change relative to cold length). This work is quite remarkable as the reported device combines fast actuation responses ~10 % s^{-1}, with significant actuation strain magnitudes (up to 30%) and high work densities (up to 40 kJ m^{-3}) – a performance similar to that of mammalian muscles. Moreover, due to the inclusion of disulfide bridges in the LCE, the actuators were shown to be resistant to delamination, self-repairable, and recyclable. Although this type of actuating device requires significant control hardware (water reservoirs, valves, and electronics), which would ideally be incorporated into a single standalone device, we believe this work is the closest to date to realize a muscle-like LCE actuator. Looking forward, one would expect that the performance of such devices could be optimized through the shape of the fluid channels and the heat capacity and thermal conductive of the chosen pump liquid.

IV. 3D printing LCEs

A. Direct ink writing

Direct ink writing (DIW) 3D printing for fabricating monodomain LCEs was first described by Ambulo *et al.* and has quickly been demonstrated as a versatile technique for processing LCEs of various functionalities and responsivities.[34] Critical to the success of DIW printed LCEs has been the ability to easily customize the molecular

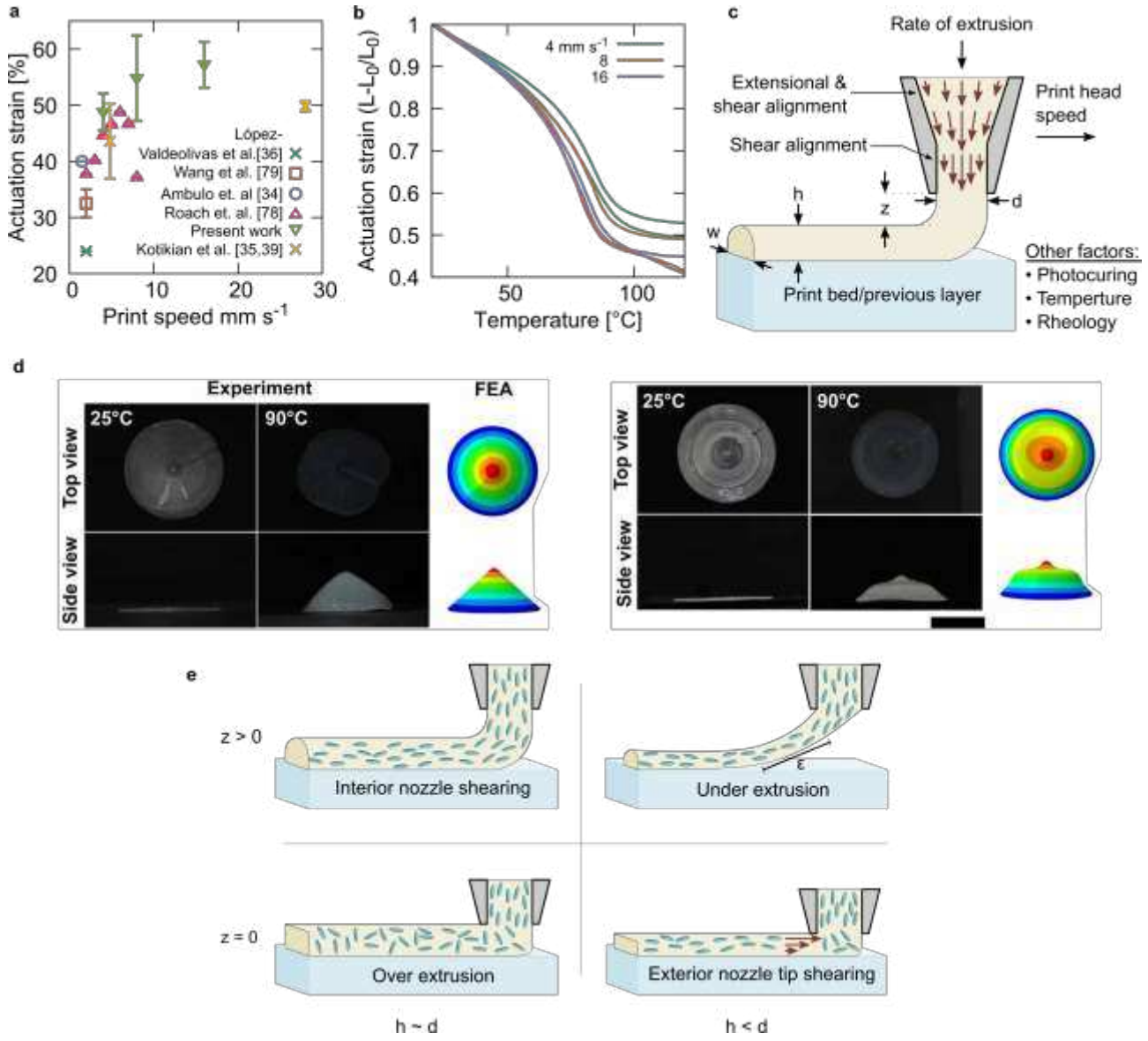

Figure 3 a *Comparisons of strain actuations vis print speed for various examples of DIW printed LCE actuators. While there the trend shows print speed has a strong influence on strain actuation and that even larger strain actuations may be possible.* ***b*** *Actuation strain vs temperature for our own experiments with a thiol acrylate-based DIW-printed LCE.* ***c*** *The quality of alignment achieved in DIW printed LCEs depends on many different chemical properties and processing conditions.* ***d*** *Wang et al. controlled LC alignment on printing using temperature and shows they can locally modulate the strain actuation in a single device – controlling the actuated shape.* ***e*** *Based on the methods and results of DIW-printed LCE studies we illustrate four examples of how print conditions can affect the alignment within printed fibers of LCE. Reprinted from Wang et al., Sci. Adv.* ***6****, eabc0034 (2020). © The Authors, some rights reserved; exclusive licensee AAAS. Distributed under a Creative Commons Attribution NonCommercial License 4.0 (CC BY-NC).*

weight, functionality, and responsivity of the photopolymerizable click-chemistry LC oligomer inks. The first reports of DIW printed LCEs showed that by extruding LC oligomers through a nozzle and depositing them on to a substrate, one could produce filaments of monodomain LCE with the director aligned parallel to the print head's movement direction.[34–36] Thermally-actuated devices, such as snap-through jumping actuators and tuneable 2D meshes, demonstrated the ability of DIW printing to produce actuators that would be difficult to fabricate through

traditional means. Moreover, through printing multilayered devices, it is now simple to create actuators with increased work capacities. For example, a printed set of LCE layers could deform an elastomeric lens and therefore modulate its focal power.

Subsequent works have introduced additional levels of responsivity and reprogrammability to DIW-printed LCE devices.[1,71,76] Above, we highlighted the work of E. Davidson *et al.,* where the use of an allyl dithiol group enabled shape fixing and alignment erasing through RAFT-mediated bond exchange .[71] In addition, Barnes *et al.* demonstrated DIW printing of a two-stage thiol acrylate LCE monomer solution into a liquid bath doped with a base Michael addition catalyst. Upon printing, the catalyst triggered the first stage's polymerization of a lightly crosslinked network. Simultaneously, the liquid bath also supported extruded filament against gravity - enabling the printing of complex features such as overhangs. Upon removal from the liquid bath, the device could then be mechanically programmed into a monodomain – locked in *via* photopolymerization of second stage crosslinks.[76] A similar approach was taken by Roach *et al*. to create aligned fibers of LCE by printing a the monomer solution onto a rotating drum, allowing the first (unaligned) network to form, and then subsequently aligning and programming of the fibers through mechanical stretching and formation of the secondary crosslinks.[77]

One of the initial core focuses of DIW printing LCEs was to maximize the actuation capacity of printed devices, with print speed often explored as a controlling variable. Fig. 3(a) collates the print speeds used and actuation strains achieved in examples of DIW printed LCEs reported to date.

Kotikian *et al.* demonstrated the nematic order parameter (well known to correlate with actuation strain) to increase from 0.31 to 0.38 for filaments extruded at 2 and 6 mm s^{-1}, respectively.[35] However, for further increases in print speed up to 10 mm s^{-1}, the order parameter remained constant. For context, far (<20°C) below the nematic-to-isotropic transition temperature, T_{NI}, nematic LCEs typically have order parameters ranging between ~0.3 and ~0.6, with the theoretical bounds of a positive order parameter being 0 and 1.[20] In their actuation tests, the authors reported a 44% actuation strains for LCEs printed at ~5 mm s^{-1}. In later works with similar chemistry, Kotikian *et al.* were able to achieve 49% actuation with a print speed of 28 mm s^{-1}.[39]

When studying a thiol-acrylate DIW-printable LCE, Roach *et al.* also demonstrated print speed to have a large effect on actuation strain.[78] The authors found an increasing actuation strain from 38 to 48 % for print speeds increasing from 2 to 6 mm s^{-1}. Interestingly, the authors found that increasing the print speed to 8 mm s^{-1} caused a decrease in actuation strain to 37%. This complicated relationship appears to be a consequence of using a constant extrusion air pressure for all printing speeds. This means the volume of material extruded per unit time remained constant despite the different travelling speeds of the print head. In our own experiments using the same LC oligomer chemistry (described in the methods), we record actuation strains of 49±3, 55±8 and 57±4 % for print speeds of 4, 8 and 16 mm s^{-1}, respectively [Figs. 3(a) and (b)]. The origin of these differences is likely to lie in the other differences in print conditions between Roach *et al.* and our own printing.

Comparing our own procedure against that of Roach *et al.,* we can identify several significant differences. Firstly, in our experiments, the volumetric flow rate is kept proportional to the print speed, ensuring that (for each print speed) the same quantity of material is deposited per unit length of printed material. Second, while we took a solvent-less approach to oligomer synthesis (see methods) and produced an oligomer with a T_{NI} of 65°C [Fig. S1], Roach *et al.* used acetone to aid the mixing of monomer components and recorded a material T_{NI} of 42°C. This lower T_{NI} suggests that the acetone was not entirely removed before printing and/or may also indicate a difference in oligomer molecular weight.

Fig. 3(c) illustrates the many variables, in addition to chemistry, which one can use to optimize and control the quality of printing and magnitude of LC order in DIW printed LCE devices. Whereas when DIW printing conventional elastomeric, many of these parameters may be redundant or irrelevant, the added complexity of controlling molecular alignment means an actuating LCE device's performance will depend on all these factors.

Wang *et al.'s* recently published study distinctly demonstrated how LC alignment and LCE actuation are highly dependent on the printing parameters highlighted by Fig. 3(c). In their work, the authors used these effects to create devices with locally-controlled actuation strains.[79] For example, by changing the extruded oligomer's temperature throughout different parts of a print, one can control the shape profile of thermally activated "popping" cones [Fig. 3(d)]. *Via* microscopy, Wang *et al.* also deduced that their printed filament was composed of a central unaligned core of oligomer surrounded by an outer aligned sheath of oligomer. The relative size of the core and sheath directly impacted the actuation strain and was dependent on the nozzle temperature, the nozzle diameter (*d* in Fig. 3(c)), and the nozzle height above the print bed (*h+z* in our Fig. 3(c)). Broadly speaking, greater actuation strains were achieved for lower printing temperatures and for smaller nozzle distances above the print bed. Their tests show that by changing print conditions, actuation strain could be tuned between ~0% to ~35%. In some instances, high actuation strains were seen for print nozzle temperatures almost ~50°C above the oligomer T_{NI} – although we would postulate that in these cases, the closeness of the nozzle to the (ambient temperature) print bed meant that only a thin and quickly cooled filament of oligomer was extruded in these cases. The authors concluded that in printing devices with spatially varying actuation strains, controlling actuation strain with temperature would be the most convenient. However, from our own experience we would suggest that changing the nozzle distance from the print bed would much be simpler, as it only requires a line of *G-code* command to move the nozzle closer or further away from the print bed, thus instantly modulating the actuation strain. By comparison, temperature changes would require the printing to pause while the ink reservoir temperature equilibrates.

The results of Wang *et al.* and others allow us to propose illustrations of how alignment can be controlled by printing conditions [Fig. 3(e)]. Relative to the nozzle diameters, the authors investigated nozzle heights to nozzle diameter ratios (*h+z*)/*d* of 0.25, 0.50, 0.75, and 1.0. From their figures and information provided in their paper, it therefore appears the typically the z-offset, *z*, was zero for many of the conditions explored. Thus according to our illustrations of alignment in Fig. 3(e), high alignment could have been achieved where the nozzle tip exterior could impart a large shear on the relatively thin layers, and low alignment established by thicker layers with lower shearing, dominated by over extrusion effects. Returning to our results, we note that we achieved high actuations strains of 48±3 % with a print speed of 4 mm s^{-1} and a *z*/*h* ratio of 0.64, while Wang *et al.'s* highest actuation of 30-35% was seen with a print speed of 2 mm s^{-1} and a z/h ratio of 0. Considering the illustrations of Fig. 3(e), we believe our notably greater actuation strains were achieved as our non-zero z-offset allowed the persistence of the shear and extensional alignments established inside the nozzle prior to extrusion. While the strain actuation in DIW printed LCEs falls short of that seen in early polysiloxane-based monodomain LCEs (up to 75%), the results of Fig. 3(a) show that through tuning materials and printing conditions, such, large actuation strains may be soon be achieved.

Zhang *et al.'s* work demonstrated further increases in complexity of liquid crystal alignment over director patterning via the print path. Their work (in contrast to all other publications known to date on DIW LCE printing) used a bespoke liquid crystal oligomer with main chain biphenyl groups and crosslinked via photodimerization of cinnamyl groups. The authors report achieving a gradient in liquid crystal ordering throughout the height of a printed filament. This gradient, perhaps not too dissimilar to the above mentioned polydomain core/monodomain sheath concept later reported by Wang *et al.*, caused the printed filaments to undergo combinations of bending and contractile actuations as opposed to the pure contractile actuation reported in other studies. Interestingly, when printing in silicone oil (intended to reduce the thermal gradient), the printed LCEs no longer exhibited the bending deformations and were purely contractile. While the results show an evident phenomenon, we believe there are open questions about the exact mechanism for this behavior, which the authors state is due to a thermal gradient across the printed filament.

Optimizing shear alignment to control actuation strain magnitude and bending/contraction behavior is clearly an exciting and unsolved challenge requiring further study from experimentation from chemical, physical, and engineering points of view. While the shear alignment behavior of liquid crystal polymers has long been studied,

much is left to be learned about the dynamics and ordering of liquid crystal polymers in DIW 3D printing, where the final alignment is dependent on the oligomer viscoelasticity, how the oligomer flows, and the various shear and extensional forces.

B. Resin-based printing

A notable limitation of DIW printing of soft and photocured elastomers is that it is difficult to produce certain features such as high aspect ratio elements (printed height >> in layer dimensions) and overhanging features. While Barnes *et al.* provided one potential solution by printing LCEs in a liquid bath, other solutions may be offered by resin-based printing technologies such as digital light process (DLP), stereolithography, and continuous liquid interface printing.

We recently described a DLP-printable LC-oligomer resin, which we used to print large (~cm^3) isotropic and anisotropic digital lattice devices with high (10µm) feature resolution.[13,37] The printed polydomain LCE devices demonstrated far greater levels of strain-rate dependency and load curve hysteresis (dissipated energy) compared to equivalent lattices printed from a conventional commercial DLP-printable elastomer resin. Our addition of toluene, used to lower the resin viscosity and which was removed post-printing, caused our resin to be an isotropic liquid. Therefore, in the system we described it seems unlikely that any monodomain alignment could be achieved.

However, monodomain DLP-printed LCEs could be possible if one were to develop a low-viscosity nematic resin which polymerizes into a soft elastomeric material. Tabrizi *et al.* recently described a DLP approach to fabricating multi-material devices with monodomain glassy LC networks as one possible component. Using a low viscosity, photo-responsive mesogenic diacrylate resin, and a strong magnet mounted on a motorized rotation plate, the authors were able to control the nematic alignment direction within the resin and selectively cure parts of devices with various monodomain orientations. The authors constructed final devices as large as ~50x50x20 mm^3, which showed actuation responsivity to thermal and optical stimuli. While the final devices were glassy LC networks and showed modest actuation compared to LCEs, we believe this work represents an important step toward freeform, high-resolution control of the LC director in arbitrarily shaped devices. Furthermore, incorporating multiple different materials into the printed objects offers a route to include elements for delivering electrical or optical actuation stimuli. Additionally, one could also imagine taking inspiration from the examples of re-processible LCE DIW printing by Barnes *et al.* and E. Davidson *et al.* to first print complex-geometry polydomain devices, which could then be mechanically programmed into monodomain actuating configurations.

V. Outlook

It is amazing to see how much LCE research has advanced over the past few years. Looking back at the 2012 review by Brommel *et al.*, the synthesis of main-chain LCEs was at that time limited to step-growth reactions using high purity monomers and careful experimental conditions.[80] Click chemistries have significantly reduced the synthetic challenges associated with main-chain LCEs, offering a facile method to tailor polymer structure and functionality. These reactions can also be scaled to create a range of thin films and large bulk devices. Moreover, the versatility of click chemistry LCEs means one can process monodomains using two-stage mechanical, surface alignment, and DIW 3D printing techniques.[22,26,34] Click-chemistries also enable the ability to easily substitute starting mesogen, spacer or crosslinking monomers to enable multiple functionalities. A traditional example of this would be the introduction of light-driven actuation by the inclusion of photo-isomer mesogens. More recent examples are click chemistries LCEs with functionalities such as dynamic networks, vitrification, and polymer crystallinity.[10,16,17,32] Some of the most recent studies which integrate these functionalities into 3D printed devices are particularly exciting developments.[1,71] In short, the ability to synthesize and tailor functional main-chain LCEs is no longer the grand challenge it used to be. The simplicity and the versatility of the synthesis route enables advance processing techniques and has allowed a diverse range of researchers of varying chemistry expertise to make their own advances in the LCE field.

A next step in the evolution of these materials is focused on the design of LCE networks. While the use of commonly available starting materials, such as RM257, RM82, and PETMP, has undoubtedly helped advance the field, their sole use in LCE systems may be preventing researchers from fully optimizing devices and exploring the contributions of mesogenic and other non-covalent interactions on LCE behaviors. From the liquid crystal displays research from which this field grew, we can plainly see how device performance is easily enhanced, optimized, and tuned by modifying the structure and mixtures of mesogenic groups. In LCEs, there are still unanswered questions with regards to how mesogenic and non-covalent interactions influence properties such as actuation rate, paranematic behavior, soft elasticity, and dissipative effects beyond traditional viscoelasticity. These interactions may be the key to improving the performance of LCEs to respond as ideal actuators and dissipators with sharp, first-order transition-like responses.

The programming of monodomains has been another traditional challenge in LCEs. In 2014, Pei *et al.* commented that uniform, well-aligned monodomains were incredibly hard to achieve in practice.[32] Voxelated surface alignment has shown an exquisite ability to expand surface anchoring techniques beyond uniformly aligned and twisted nematic monodomains. This technique has shown incredibly high resolution but is generally limited to thin films. 3D printing has emerged as a robust manufacturing technique that offers fine resolution (10 – 100 μm) while maintaining the ability to fabricate bulk devices. DIW has been shown to be the most accessible additive method to align monodomains inherently through shearing effects possible with every DIW printer. In contrast, current DLP and stereolithography printers require special modification to control alignment through magnetic fields.

Two of the main benefits of additive manufacturing are the ability to create structures and geometries that would otherwise be impossible, and the ability to easily create complex devices from multiple material types. We hope that these key benefits of additive manufacturing will soon be exploited in LCEs research. For example, in the pursuit of bulk, muscle-like actuators, additive manufacturing could enable the fabrication of devices where actuating stimuli and power can be effectively applied and removed throughout the bulk of a device by use of networks of channels or wires. As muscles themselves have such structures (additively manufactured by biology!), we are optimistic that truly muscle-like actuators will be developed with 3D printing.

Despite all the recent processing advances described in this perspective, we note that all the techniques for voxelated LCE alignment generally exhibit 2D freedom control of the director within a 2D plane of material. Arbitrary 3D freeform control of voxelated director configurations in bulk devices is yet to be realized – although we acknowledge that many applications could already be realized without such complete control over the LC director.

LCEs with dynamic chemistries have opened multiple new opportunities to increase functionality as well as to investigate structure-property relationships. LCEs are most commonly reported as artificial muscles; however, muscles have functionality beyond actuation. For example, muscles can be trained to learn new tasks, repair themselves when damaged, and change their modulus (e.g., flexing). Dynamic network chemistries enable many of these same responses in LCEs and may offer the ability to truly mimic muscle behavior.

Such networks also provide a unique way to explore structure-property relationships in LCEs through erasing a network's synthetic history or reprogramming its order. Research has shown that the synthetic history of a LCE, that is whether the network is formed in the nematic or isotropic state, can influence the actuation, mechanical and optical properties of a LCE.[20,31,81] For example, a monodomain sample prepared *via* mechanical stretching would have polymer chains aligned with the director. Using a bond-exchange reaction, the monodomain could be preserved while relaxing the polymer chains to a high-entropy ground state. Such an approach would allow us to separate the contributions of the network entropy and liquid crystalline order on the actuation dynamics and mechanical properties of a single system.

As we enter the second century of polymers research, the polymers community is required to integrate sustainability, renewability, and recyclability into the novel highly functional materials it continues to innovate. Recent developments in dynamic and bond exchangeable LCE networks have shown that LCEs can meet these requirements. However, the use of such materials in LCEs research is not yet standard. Just as click-chemistries have opened up LCEs research to wider communities, we hope that the coming few years will see synthesis of renewable and recyclable LCEs becoming equally as facile as thermoset LCEs. If the use of sustainable LCEs becomes the norm, then the anticipated commercial LCE devices will be renewable and recyclable from the outset.

Looking forward, we are excited by recent research showing that innovation in the processing, stimulation and actuation of LCEs is ever continuing. For example Wei *et al*. recently demonstrated a simple, self-assembled route to the creation of fractal-like structures from LC-networks – structures with a resolution and complexity which may be even be difficult to achieve via additive manufacturing.[82] While no actuation of the final polymerized structures was demonstrated, the processing technique is truly inspirational for future LCE research. In addition, the recent report of negative order parameters in LCEs adds new actuation modes to LCEs beyond those which have been studied for the last half century.[8,83]Zeng *et al*.'s report of Pavlovian-inspired learning and conditioning of LC network actuators demonstrates new avenues to enhance the multifunctionality, programmability and smartness of LCE devices.[84] Lastly, Zuo *et al.* have demonstrated adding additional color-changing responsivity to actuating LCEs via photo- and thermo-chromic effects. This added responsivity introduces visual and self-reporting functionality to the state of a LCE actuator which could be applicable to camouflage, consumer, and architectural technologies.[85]

The focus of this perspective has been to highlight recent advances in LCEs with an emphasis in actuation. As is clear, LCEs show great promise in the field of active polymers, especially since LCE actuators are often reported with actuation strains and work capacities greater than those of mammalian muscles. With the recent advancements in synthesis and manufacturing, researchers now have multiple avenues to create bespoke devices with tailored alignment and actuation response. The LCE community should be mindful to realize the potential of these materials.

To date, LCEs have not experienced widespread adoption or high-value commercial success in comparison to other active materials, such as shape-memory polymers (SMPs) and alloys. For example, heat shrink tubing, which is made from SMPs, is a commodity product widely used in electronics wiring. In addition, Shape Memory Medical, Inc. (Santa Clara, CA, USA) has developed a line of SMP embolization devices, which have received CE marking. The shape-memory effect in nickel-titanium alloys has been also used in a variety of orthopedic and cardiovascular devices. Overall, these examples demonstrate that there are market opportunities for active materials and should be highly encouraging to LCE researchers.

By comparison, LCEs have yet to be proven safe and effective in biomedical devices. For robotic applications, decreasing response time and increasing the power of LCEs is of high importance, and may be a new set of barriers to the field. Moving forward, simply demonstrating actuation behavior will be insufficient in novelty. Researchers will need to design LCEs as a material, device, and system to meet the requirements of specific proposed applications (e.g., biocompatibility, response time, actuation method, etc.). Admittedly, this perspective does not fully cover other unique properties in LCEs such as soft elasticity, mechanical energy dissipation, or optical properties – areas where fewer barriers to commercialization may exist.

In summary, the field of LCE research possesses an exciting future. Based on the literature published over the past decade, advancements related to chemistries, manufacturing techniques, functionalities, and proposed applications are being made at an increasingly rapid pace. As authors, we believe that LCEs have the potential to be as commercially successful as liquid crystals were in displays. The field is at a point where such breakthroughs scientifically and commercially are within are reach over the next decade.

Materials and methods

Acrylate-capped LC oligomers were synthesized using 4-(3-acryloyloxypropyloxy)benzoic acid 2-methyl-1,4-phenylene ester (RM257, CAS 174063-87-7), 2,2'-(ethylenedioxy)diethanethiol (EDDT, CAS 4970-87-7), butylated hydroxytoluene (BHT, CAS 128-37-0), 2-Hydroxy-4'-(2-hydroxyethoxy)-2-methylpropiophenone (HHMP, CAS 106797-53-9) and N,N,N',N'',N''-Pentamethyldiethylenetriamine (PMDETA, CAS 3030-47-5). RM257 was purchased from Wilshire Technologies, all other components were purchased from Sigma Aldrich and all components were used as received.

Liquid crystalline oligomers were synthesized via the thiol-Michael click-reaction, described in detail elsewhere.[1] Briefly, BHT (radical-inhibitor, 1.4 mol. % of total reactants, typically 0.090 g), RM257 (diacrylate mesogenic monomer, 51.1 mol. %, 9.00 g) and HHMP (UV-radical photoinitiator, 1.9 mol. %, 0.124 g) were added to a glass vial and melted together in a water bath set at 70°C. The melted components were thoroughly mixed before EDDT (dithiol spacer monomer, 44.4 mol. %, 2.49 g) and PMDETA (base catalyst, 1.2 mol. %, 0.060 g) were added and the mixture mixed and degassed. The mixture was then transferred to the DIW-printing barrels and left in an oven set at 70°C for half an hour to start the Michael addition. The barrel was then left at ambient temperature and protected from light for 2 days before printing. The chosen ratio of RM257:EDDT (1.15:1) ensured oligomers were acrylate capped and therefore would undergo crosslinking during 3D printing.

DIW printing was performed using a Hyrel Engine HR 3D printer equipped with a KRA-2 print head for heating and extruding LC oligomers along directed print paths. Barrels containing printable oligomer were installed in the KRA print head which was set at 65°C for the LC-ink (left for an hour prior to printing for equilibration). During printing, materials were extruded through a Tecdia Arque-S 5060 nozzle which had an internal diameter of 500 µm at the nozzle tip. *g-code* toolpaths controlling the print head's motion, printer settings and volumetric rate of material extrusion were created using in-house developed python scripts. Films three layers thick were printed for actuation tests. During extrusion, the extruded material was exposed to UV light to trigger crosslinking of the LCE. Post-printing, the films (typically 20 x 30 x 1 mm) were fully cured through exposure to high intensity UV light in a UVP CL-1000 (Ultraviolet Crosslinkers, Upland, CA, USA) chamber for 15 minutes on each side.

Strips of LCE, approximately 5 mm wide, were cut with their long edge parallel to the print path and LC director which were tested using a TA Instruments Q800 dynamic mechanical analyzer. During cooling temperature sweeps from 130°C, the length of the films was monitored using 1 Hz strain oscillations of 0.1% strain amplitude. Throughout testing films were kept taught as they were mounted using a small 0.01 N preload force (2 kPa stress) and overstraining was avoided through force tracking at 120% to account for the changing modulus with temperature. Strain actuation was calculated from the length change of the LCE strip relative to the length at room temperature.

Supplemental Material

See Supplemental Material for DSC information on liquid-crystal oligomers for 3D printing.

Acknowledgements

This material was based upon work supported by, or in part by, the U.S. Army Research Laboratory and the U. S. Army Research Office under grant number W911NF1710165. This work was also supported under NSF CAREER Award 1350436, NSF PFI Award 1827288, NSF Award 1901807, and by the Laboratory Directed Research and Development program at Sandia National Laboratories, a multi-mission laboratory managed and operated by National Technology & Engineering Solutions of Sandia, LLC, a wholly owned subsidiary of Honeywell International Inc., for the U.S. Department of Energy's National Nuclear Security Administration under contract DE- NA0003525. Devesh Mistry would like to thank the English Speaking Union for support through the Lindemann Trust Fellowship.

Declaration of Competing Interest

CMY has a financial interest in a company, Impressio Inc., trying to commercialize LCE products.

References

[1] R.H. Volpe, D. Mistry, V. V. Patel, R.R. Patel, and C.M. Yakacki, Adv. Healthc. Mater. **9**, 1901136 (2020).

[2] T.J. White and D.J. Broer, Nat. Mater. **14**, 1087 (2015).

[3] R.S. Kularatne, H. Kim, J.M. Boothby, and T.H. Ware, J. Polym. Sci. Part B Polym. Phys. **55**, 395 (2017).

[4] S.W. Ula, N.A. Traugutt, R.H. Volpe, R.R. Patel, K. Yu, and C.M. Yakacki, Liq. Cryst. Rev. **6**, 78 (2018).

[5] H. Zeng, O.M. Wani, P. Wasylczyk, R. Kaczmarek, and A. Priimagi, Adv. Mater. **29**, 1701814 (2017).

[6] W. Feng, D.J. Broer, and D. Liu, Adv. Mater. **30**, 1704970 (2018).

[7] M.E. Prévôt, H. Andro, S.L.M.M. Alexander, S. Ustunel, C. Zhu, Z. Nikolov, S.T. Rafferty, M.T. Brannum, B. Kinsel, L.T.J.J. Korley, E.J. Freeman, J.A. McDonough, R.J. Clements, and E. Hegmann, Soft Matter **14**, 354 (2018).

[8] D. Mistry, S.D. Connell, S.L. Mickthwaite, P.B. Morgan, J.H. Clamp, H.F. Gleeson, S.L. Micklethwaite, P.B. Morgan, J.H. Clamp, and H.F. Gleeson, Nat. Commun. **9**, 5095 (2018).

[9] A.M. Flatae, M. Burresi, H. Zeng, S. Nocentini, S. Wiegele, C. Parmeggiani, H. Kalt, and D. Wiersma, Light Sci. Appl. **4**, e282 (2015).

[10] M.O. Saed, R.H. Volpe, N.A. Traugutt, R. Visvanathan, N.A. Clark, and C.M. Yakacki, Soft Matter **13**, 7537 (2017).

[11] D.W. Hanzon, N.A. Traugutt, M.K. McBride, C.N. Bowman, C.M. Yakacki, and K. Yu, Soft Matter **14**, 951 (2018).

[12] Z. Wang, Q. He, Y. Wang, and S. Cai, Soft Matter **15**, 2811 (2019).

[13] N.A. Traugutt, D. Mistry, C. Luo, K. Yu, Q. Ge, and C.M. Yakacki, Adv. Mater. **32**, 2000797 (2020).

[14] M.K. McBride, A.M. Martinez, L. Cox, M. Alim, K. Childress, M. Beiswinger, M. Podgorski, B.T. Worrell, J. Killgore, and C.N. Bowman, Sci. Adv. **4**, eaat4634 (2018).

[15] M.O. Saed and E.M. Terentjev, ACS Macro Lett. 749 (2020).

[16] M.O. Saed, A. Gablier, and E.M. Terentejv, Adv. Funct. Mater. **30**, 1906458 (2020).

[17] Z. Wang and S. Cai, J. Mater. Chem. B **8**, 6610 (2020).

[18] M.O. Saed, A. Gablier, and E.M. Terentjev, Chem. Rev. acs. chemrev.0c01057 (2021).

[19] Y. Zhang, Z. Wang, Y. Yang, Q. Chen, X. Qian, Y. Wu, H. Liang, Y. Xu, Y. Wei, and Y. Ji, Sci. Adv. **6**, eaay8606 (2020).

[20] M. Warner and E.M. Terentjev, *Liquid Crystal Elastomers* (Clarendon Press, Oxford, 2013).

[21] L.T. de Haan, C. Sánchez-Somolinos, C.M.W. Bastiaansen, A.P.H.J. Schenning, and D.J. Broer, Angew. Chemie Int. Ed. **51**, 12469 (2012).

[22] T.H. Ware, M.E. McConney, J.J. Wie, V.P. Tondiglia, and T.J. White, Science. **347**, 982 (2015).

[23] C.D. Modes, M. Warner, C. Sánchez-Somolinos, L.T. de Haan, and D. Broer, Phys. Rev. E **86**, 060701 (2012).

[24] C. Mostajeran, M. Warner, and C.D. Modes, Soft Matter **13**, 8858 (2017).

[25] J. Küpfer and H. Finkelmann, Die Makromol. Chemie, Rapid Commun. **12**, 717 (1991).

[26] C.M. Yakacki, M. Saed, D.P. Nair, T. Gong, S.M. Reed, and C.N. Bowman, RSC Adv. **5**, 18997 (2015).

564 [27] K. Urayama, Y.O. Arai, and T. Takigawa, Macromolecules **38**, 3469 (2005).

565 [28] Y. Xia, E. Lee, H. Hu, M.A. Gharbi, D.A. Beller, E.-K. Fleischmann, R.D. Kamien, R. Zentel, and S. Yang, ACS Appl.
566 Mater. Interfaces **8**, 12466 (2016).

567 [29] S. Schuhladen, F. Preller, R. Rix, S. Petsch, R. Zentel, and H. Zappe, Adv. Mater. **26**, 7247 (2014).

568 [30] M. Tabrizi, T.H. Ware, and M.R. Shankar, ACS Appl. Mater. Interfaces **11**, 28236 (2019).

569 [31] N.A. Traugutt, R.H. Volpe, M.S. Bollinger, M.O. Saed, A.H. Torbati, K. Yu, N. Dadivanyan, and C.M. Yakacki, Soft
570 Matter **13**, 7013 (2017).

571 [32] Z. Pei, Y. Yang, Q. Chen, E.M. Terentjev, Y. Wei, and Y. Ji, Nat. Mater. **13**, 36 (2014).

572 [33] H. Zeng, P. Wasylczyk, C. Parmeggiani, D. Martella, M. Burresi, and D.S. Wiersma, Adv. Mater. **27**, 3883 (2015).

573 [34] C.P. Ambulo, J.J. Burroughs, J.M. Boothby, H. Kim, M.R. Shankar, and T.H. Ware, ACS Appl. Mater. Interfaces **9**,
574 37332 (2017).

575 [35] A. Kotikian, R.L. Truby, J.W. Boley, T.J. White, and J.A. Lewis, Adv. Mater. **30**, 1706164 (2018).

576 [36] M. López-Valdeolivas, D. Liu, D.J. Broer, and C. Sánchez-Somolinos, Macromol. Rapid Commun. **39**, 1700710
577 (2018).

578 [37] C. Luo, C. Chung, N.A. Traugutt, C.M. Yakacki, K.N. Long, and K. Yu, ACS Appl. Mater. Interfaces acsami.0c17538
579 (2020).

580 [38] C.P. Ambulo, S. Tasmim, S. Wang, M.K. Abdelrahman, P.E. Zimmern, and T.H. Ware, J. Appl. Phys. **128**, 140901
581 (2020).

582 [39] A. Kotikian, C. McMahan, E.C. Davidson, J.M. Muhammad, R.D. Weeks, C. Daraio, and J.A. Lewis, Sci. Robot. **4**,
583 eaax7044 (2019).

584 [40] J.D.W. Madden, N.A. Vandesteeg, P.A. Anquetil, P.G.A. Madden, A. Takshi, R.Z. Pytel, S.R. Lafontaine, P.A.
585 Wieringa, and I.W. Hunter, IEEE J. Ocean. Eng. **29**, 706 (2004).

586 [41] P. Brochu and Q. Pei, Macromol. Rapid Commun. **31**, 10 (2010).

587 [42] Q. He, Z. Wang, Y. Wang, A. Minori, M.T. Tolley, and S. Cai, Sci. Adv. **5**, eaax5746 (2019).

588 [43] S. Courty, J. Mine, A.R. Tajbakhsh, and E.M. Terentjev, Europhys. Lett. **64**, 654 (2003).

589 [44] T. Guin, B.A. Kowalski, R. Rao, A.D. Auguste, C.A. Grabowski, P.F. Lloyd, V.P. Tondiglia, B. Maruyama, R.A. Vaia,
590 and T.J. White, ACS Appl. Mater. Interfaces **10**, 1187 (2018).

591 [45] T. Guin, H.E. Hinton, E. Burgeson, C.C. Bowland, L.T. Kearney, Y. Li, I. Ivanov, N.A. Nguyen, and A.K. Naskar, Adv.
592 Intell. Syst. **2**, 2000022 (2020).

593 [46] K. Urayama, S. Honda, and T. Takigawa, Macromolecules **38**, 3574 (2005).

594 [47] T. Okamoto, K. Urayama, and T. Takigawa, Soft Matter **7**, 10585 (2011).

595 [48] Z.S. Davidson, H. Shahsavan, A. Aghakhani, Y. Guo, L. Hines, Y. Xia, S. Yang, and M. Sitti, Sci. Adv. **5**, eaay0855
596 (2019).

597 [49] J. Liu, Y. Gao, H. Wang, R. Poling-Skutvik, C.O. Osuji, and S. Yang, Adv. Intell. Syst. **2**, 1900163 (2020).

598 [50] M.J. Ford, M. Palaniswamy, C.P. Ambulo, T.H. Ware, and C. Majidi, Soft Matter **16**, 5878 (2020).

599 [51] T.A. Kent, M.J. Ford, E.J. Markvicka, and C. Majidi, Multifunct. Mater. **3**, 025003 (2020).

[52] C.P. Ambulo, M.J. Ford, K. Searles, C. Majidi, and T.H. Ware, ACS Appl. Mater. Interfaces acsami.0c19051 (2020).

[53] D. Liu, N.B. Tito, and D.J. Broer, Nat. Commun. **8**, 1526 (2017).

[54] L. Dong and Y. Zhao, Mater. Chem. Front. **2**, 1932 (2018).

[55] M. Yamada, M. Kondo, J. Mamiya, Y. Yu, M. Kinoshita, C.J. Barrett, and T. Ikeda, Angew. Chemie Int. Ed. **47**, 4986 (2008).

[56] O.M. Wani, H. Zeng, and A. Priimagi, Nat. Commun. **8**, 1 (2017).

[57] L. Ceamanos, Z. Kahveci, M. López-Valdeolivas, D. Liu, D.J. Broer, and C. Sánchez-Somolinos, ACS Appl. Mater. Interfaces **12**, 44195 (2020).

[58] A.H. Gelebart, D. Jan Mulder, M. Varga, A. Konya, G. Vantomme, E.W. Meijer, R.L.B. Selinger, and D.J. Broer, Nature **546**, 632 (2017).

[59] T.F. Scott, Science **308**, 1615 (2005).

[60] T.F. Scott, R.B. Draughon, and C.N. Bowman, Adv. Mater. **18**, 2128 (2006).

[61] D. Montarnal, M. Capelot, F. Tournilhac, and L. Leibler, Science **334**, 965 (2011).

[62] M. Capelot, D. Montarnal, F. Tournilhac, and L. Leibler, J. Am. Chem. Soc. **134**, 7664 (2012).

[63] Y. Jin, C. Yu, R.J. Denman, and W. Zhang, Chem. Soc. Rev. **42**, 6634 (2013).

[64] P. Taynton, K. Yu, R.K. Shoemaker, Y. Jin, H.J. Qi, and W. Zhang, Adv. Mater. **26**, 3938 (2014).

[65] N. Ponnuswamy, F.B.L. Cougnon, J.M. Clough, G.D. Pantos, and J.K.M. Sanders, Science **338**, 783 (2012).

[66] J. Li, J.M.A. Carnall, M.C.A. Stuart, and S. Otto, Angew. Chemie Int. Ed. **50**, 8384 (2011).

[67] M.O. Saed and E.M. Terentjev, Sci. Rep. **10**, 17 (2020).

[68] M.K. McBride, M. Hendrikx, D. Liu, B.T. Worrell, D.J. Broer, and C.N. Bowman, Adv. Mater. **29**, (2017).

[69] Z. Wang, H. Tian, Q. He, and S. Cai, ACS Appl. Mater. Interfaces **9**, 33119 (2017).

[70] X. Qian, Q. Chen, Y. Yang, Y. Xu, Z. Li, Z. Wang, Y. Wu, Y. Wei, and Y. Ji, Adv. Mater. **30**, 1801103 (2018).

[71] E.C. Davidson, A. Kotikian, S. Li, J. Aizenberg, and J.A. Lewis, Adv. Mater. **32**, 1905682 (2020).

[72] Y. Li, O. Rios, J.K. Keum, J. Chen, and M.R. Kessler, ACS Appl. Mater. Interfaces **8**, 15750 (2016).

[73] B. Ni, H.-L. Xie, J. Tang, H.-L. Zhang, and E.-Q. Chen, Chem. Commun. **52**, 10257 (2016).

[74] Z. Jiang, Y. Xiao, L. Yin, L. Han, and Y. Zhao, Angew. Chemie Int. Ed. **59**, 4925 (2020).

[75] Q. He, Z. Wang, Y. Wang, Z. Song, and S. Cai, ACS Appl. Mater. Interfaces **12**, 35464 (2020).

[76] M. Barnes, S.M. Sajadi, S. Parekh, M.M. Rahman, P.M. Ajayan, and R. Verduzco, ACS Appl. Mater. Interfaces **12**, 28692 (2020).

[77] D.J. Roach, C. Yuan, X. Kuang, V.C.F. Li, P. Blake, M.L. Romero, I. Hammel, K. Yu, and H.J. Qi, ACS Appl. Mater. Interfaces **11**, 19514 (2019).

[78] D.J. Roach, X. Kuang, C. Yuan, K. Chen, and H.J. Qi, Smart Mater. Struct. **27**, 125011 (2018).

[79] Z. Wang, Z. Wang, Y. Zheng, Q. He, Y. Wang, and S. Cai, Sci. Adv. **6**, eabc0034 (2020).

[80] F. Brömmel, D. Kramer, and H. Finkelmann, Adv. Polym. Sci. **250**, 1 (2012).

[81] H.E. Fowler, B.R. Donovan, J.M. McCracken, F. López Jiménez, and T.J. White, Soft Matter **16**, 330 (2020).

[82] W. Wei, Y. Xia, S. Ettinger, S. Yang, and A.G. Yodh, Nature **576**, 433 (2019).

[83] V.S.R. Jampani, R.H. Volpe, K. Reguengo de Sousa, J. Ferreira Machado, C.M. Yakacki, and J.P.F. Lagerwall, Sci. Adv. **5**, eaaw2476 (2019).

[84] H. Zeng, H. Zhang, O. Ikkala, and A. Priimagi, Matter **2**, 194 (2020).

[85] B. Zuo, M. Wang, B.P. Lin, and H. Yang, Chem. Mater. **30**, 8079 (2018).